Performance of Path-Time Codes for End-to-End Transmission in Ad Hoc Multihop Networks

I-Wei Lai[†], Chia-Han Lee[†], Kwang-Cheng Chen[‡], and Ezio Biglieri[§]

[†]Research Center for Information Technology Innovation
Academia Sinica, Taipei, Taiwan

[‡]Department of Electrical Engineering and Graduate Institute of Communication Engineering
National Taiwan University, Taipei, Taiwan

[§]Universitat Pompeu Fabra, Barcelona, Spain, and King Saud University, Riyadh, KSA

***Abstract*—In this paper, we study the performance of the recently proposed class of path-time codes (PTCs), which exploit time and path diversity to increase the reliability of end-to-end transmission in ad hoc multihop networks. Using the central limit theorem, we prove that PTCs reshape the statistics of a relay path including multiple cascaded links. In particular, as the number K of relay paths becomes large, the cascaded channel statistic is transformed from K-product Rayleigh to Rayleigh. This is numerically demonstrated and analytically verified by using the concept of "amount of fading" (AF). Our results show that, by using PTCs, the end-to-end error-rate performance can be boosted in addition to the diversity and coding gains.**

I. Introduction

Recently, physical-layer multiple-input multiple-output (MIMO) techniques are being applied to enhance the performance of end-to-end transmission, using for example distributed space–time code (STCs) [1]–[4] or distributed spatial multiplexing [5]. In [6], [7], the application of *virtual MIMO* technology to the network/session layer was proposed for ad hoc cognitive radio networks. By encoding packets along both path and time coordinates, path–time codes (PTCs) allow error-resilient end-to-end transmission based on multipath routing [8], [9]. The data packet is encoded to multiple PTC-coded packets and transmitted through multihop and multipath routes. These coded packets are then jointly decoded at the destination node.

Since this virtual MIMO on top of the physical layer is a new scenario for the coding theory, in this paper, we analyze the performance of end-to-end PTC transmission. We call *link* the connection between two nodes, and *path* the connection route between source and destination nodes, i.e., the end-to-end connection. By assuming that the link gains can be modeled as Rayleigh random variables, the channel of a relay path comprising multiple cascaded links has a *K-product Rayleigh* distribution. In this work, we first show that the fading of end-to-end PTC transmission is effectively modeled by the weighted sum of multiple K-product Rayleigh random variables. Using the central limit theorem, as the number of relay paths gets large, this statistic can be approximated by a Rayleigh distribution. Next, we investigate the *amount of fading* (AF) [10], which is often used to quantify the severity of the fading channel. As the number of links cascaded in the relay path increases, the AF of the K-product Rayleigh fading channel exponentially increases, implying that the communication over the cascaded fading channel has a worse error performance than over the Rayleigh fading channel. However, when a PTC is used, as the number of relay paths increases the AF of the end-to-end channel approaches that of Rayleigh fading. We derive a closed-form expression of AF for the end-to-end path–time coded channel, which shows that PTCs not only increase diversity and coding gains, but also mitigate the performance degradation caused by multihop transmission. We conclude that PTCs yield a promising technique for application to networks using *amplify-and-forward* relays.

This paper is organized as follows. Section II describes end-to-end path–time coded transmission. Section III theoretically analyzes the AF of end-to-end PTC transmission over cascaded fading channels. In Section IV, numerical results are provided to validate the analysis and demonstrate the performance of the PTC. Finally, conclusions are drawn in Section V.

II. System Model

In this work, we consider multihop networking with R link-disjoint paths [11], [12] each including $K_r - 1$ relay nodes, $r \in \{1, \ldots, R\}$, as illustrated by an equivalent directed-graph model of Fig. 1. Such multihop/multipath routing can be established using the algorithms from [8], [9].

The source node encodes a data packet $\mathbf{x} \in \chi^B$ using a permutation or discrete-Fourier-transform (DFT) code matrix $\mathbf{C}_b \in \mathbb{C}^{R \times B}$ for $b = 1, \ldots, B$ [6], [7], where χ is the signal constellation set, and B the number of coded packets used to transmit a source data packet. The resulting coded packet $\mathbf{s}_b = \mathbf{C}_b \mathbf{x}$ at time instant b is then transmitted through different relay paths by applying multiplexing techniques or a two-step protocol [3]. The coded packet in each relay path is amplified-and-forwarded toward the destination node.

978-1-4799-5186-4/14/$31.00 ©2014 IEEE

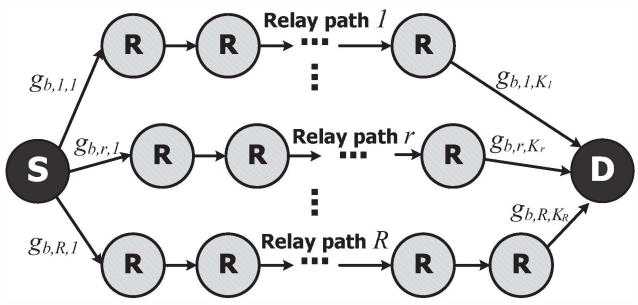

Fig. 1. Equivalent topology of the multipath end-to-end transmission in an ad hoc multihop network.

Define $\mathbf{h}_b = [h_{b,1}, \ldots, h_{b,R}]^\top \in \mathbb{C}^R$ as the vector of fading gains affecting the relay paths at time instant b, where $(\cdot)^\top$ denotes transposition. The rth entry of $\mathbf{h}_b$ is given by

$$h_{b,r} = \prod_{k=1}^{K_r} g_{b,r,k}, \tag{1}$$

where $g_{b,r,k}$ is the fading gain of the kth link in path r at time b, and K_r is the number of links in the rth relay path. We assume that the link gains are independent and identically distributed (i.i.d.) with zero mean and variance σ_g^2. It can be seen that the path fading $h_{b,r}$, obtained by cascading K_r links, yields a worse error rate performance than with systems operating over a Rayleigh fading channel [10].

The received coded packet at the destination node has the expression

$$y_b = \mathbf{h}_b^\top \mathbf{C}_b \mathbf{x} + \sum_{r=1}^{R} \tilde{n}_{b,r} = \mathbf{h}_b \mathbf{s}_b + n_b, \tag{2}$$

where $\tilde{n}_{b,r}$, the additive white Gaussian noise (AWGN) aggregated from all links in path r at time instant b, has a variance depending on both r and b, due to the amplification of the link gains [3]. Therefore, the AWGN n_b has a time-varying noise power spectral density, denoted $N_{0,b}$. The received coded packets from $b = 1$ to $b = B$ can be represented in the form

$$\mathbf{y} = \underbrace{\begin{bmatrix} \mathbf{h}_1^\top & \ldots & \mathbf{0}^\top \\ \vdots & \ddots & \vdots \\ \mathbf{0}^\top & \ldots & \mathbf{h}_B^\top \end{bmatrix}}_{\mathbf{H}} \underbrace{\begin{bmatrix} \mathbf{s}_1 \\ \vdots \\ \mathbf{s}_B \end{bmatrix}}_{\mathbf{s}} + \underbrace{\begin{bmatrix} n_1 \\ \vdots \\ n_B \end{bmatrix}}_{\mathbf{n}} = \mathbf{H}\mathbf{s} + \mathbf{n}. \tag{3}$$

With the formulation in (3), the end-to-end coded transmission in ad hoc multihop networks is described by the same mathematical expression as a MIMO system, where multiple nodes are coordinated to form multihop/multipath routes between a source/destination node pair. The source node encodes the data along time and path coordinates, then transmits the coded packets $\mathbf{s}_b$. At the destination node, multiple PTC-coded packets arriving at the destination node from various time slots and relay paths are collected and jointly decoded to recover the data packet $\mathbf{x}$. For more details of the PTC design, see [6], [7].

III. Analysis of Effective Fading

In this section, we show that in addition to the diversity and coding gains provided by conventional STCs over the Rayleigh fading channel, PTCs can reshape the statistics of the cascaded channel to a Rayleigh distribution, thereby improving the error rate performance. We prove this by deriving the pairwise error probability (PEP) and exhibiting numerical examples validating our analysis. AF calculations further elucidate this phenomenon, and show the dependence of AF on the number of relay paths and the number of links.

A. PEP Analysis

Denoting the transmitted coded packet and the erroneously detected coded packet by $\mathbf{s}$ and $\hat{\mathbf{s}}$, respectively, the PEP $f(\mathbf{s}, \hat{\mathbf{s}})$ is defined as

$$f(\mathbf{s}, \hat{\mathbf{s}}) = P\left(\Lambda(\mathbf{s}, \hat{\mathbf{s}}) < 0\right) \tag{4}$$

where Λ denotes the log-likelihood ratio (LLR) of $p(\mathbf{y} \mid \mathbf{s})$ and $p(\mathbf{y} \mid \hat{\mathbf{s}})$, i.e.,

$$\Lambda = \log p(\mathbf{y} \mid \mathbf{s}) - \log p(\mathbf{y} \mid \hat{\mathbf{s}}) \tag{5}$$

with

$$p(\mathbf{y} \mid \mathbf{s}) = \frac{1}{\pi^B \prod_{b=1}^{B} N_{0,b}} e^{-\|\mathrm{diag}(\boldsymbol{\rho})\mathbf{y} - \mathrm{diag}(\boldsymbol{\rho})\mathbf{H}\mathbf{s}\|^2}, \tag{6}$$

where $\mathrm{diag}(\boldsymbol{\rho})$ is a diagonal matrix whose diagonal entries are $\boldsymbol{\rho} = [1/\sqrt{N_{0,1}}, \ldots, 1/\sqrt{N_{0,B}},]^\top$. Inserting (6) into (5), we have

$$\begin{aligned} \Lambda &= \|\mathrm{diag}(\boldsymbol{\rho})\mathbf{y} - \mathrm{diag}(\boldsymbol{\rho})\mathbf{H}\tilde{\mathbf{s}}\|^2 - \|\mathrm{diag}(\boldsymbol{\rho})\mathbf{y} - \mathrm{diag}(\boldsymbol{\rho})\mathbf{H}\mathbf{s}\|^2 \\ &= \|\mathrm{diag}(\boldsymbol{\rho})\mathbf{H}(\mathbf{s} - \hat{\mathbf{s}})\|^2 + 2\,\mathrm{Re}\left\{\mathrm{diag}(\boldsymbol{\rho})\mathbf{H}(\mathbf{s} - \hat{\mathbf{s}})^H \mathbf{n}\right\}, \end{aligned} \tag{7}$$

showing that, given $\mathbf{H}$, Λ is a conditionally Gaussian random variable with mean

$$\mu_\Lambda = \|\mathrm{diag}(\boldsymbol{\rho})\mathbf{H}(\mathbf{s} - \hat{\mathbf{s}})\|^2 \tag{8}$$

and variance

$$\sigma_\Lambda^2 = 2\mu_\Lambda. \tag{9}$$

The conditional moment-generating function (MGF) of this Gaussian random variable Λ is given by

$$M_\Lambda(t \mid \mathbf{H}) = e^{(t+t^2)\mu_\Lambda}. \tag{10}$$

To prove (10), we reformulate μ_Λ in (8) as

$$\begin{aligned} \mu_\Lambda &= \sum_{b=1}^{B} \frac{1}{N_{0,b}} \mathbf{h}_b^H (\mathbf{s}_b^* - \hat{\mathbf{s}}_b^*)(\mathbf{s}_b - \hat{\mathbf{s}}_b)^\top \mathbf{h}_b \\ &\overset{(a)}{=} \sum_{b=1}^{B} \frac{1}{N_{0,b}} \mathbf{h}_b^H \mathbf{U}_b \mathbf{D}_b \mathbf{U}_b^H \mathbf{h}_b \\ &\overset{(b)}{=} \sum_{b=1}^{B} \frac{1}{N_{0,b}} \mathbf{v}_b^H \mathbf{D}_b \mathbf{v}_b \\ &\overset{(c)}{=} \sum_{b=1}^{B} \frac{1}{N_{0,b}} |w_b|^2 \|\mathbf{s}_b - \hat{\mathbf{s}}_b\|^2, \end{aligned} \tag{11}$$

where $(\cdot)^H$ and $(\cdot)^*$ denote Hermitian conjugation and conjugation, respectively. In (11), (a) is due to the eigendecomposition of the Hermitian matrix $(\mathbf{s}_b^* - \hat{\mathbf{s}}_b^*)(\mathbf{s}_b - \hat{\mathbf{s}}_b)^\top$ [13], while $\mathbf{U}_b$ is a unitary matrix and $\mathbf{D}_b$ is the diagonal matrix with eigenvalues being the diagonal terms; (b) is due to the definition of $\mathbf{v}_b = \mathbf{U}_b^H \mathbf{h}_b$; (c) holds because due to the rank-1 property of $(\mathbf{s}_b^* - \hat{\mathbf{s}}_b^*)(\mathbf{s}_b - \hat{\mathbf{s}}_b)^\top$, $\mathbf{D}_b$ has at most one nonzero eigenvalue, whose value is $\|\mathbf{s}_b - \hat{\mathbf{s}}_b\|^2$. Moreover, we define w_b as the entry of $\mathbf{v}_b$ associated with the nonzero eigenvector

$$w_b = \mathbf{u}_b^H \mathbf{h}_b, \tag{12}$$

where $\|\mathbf{u}_b\|^2 = 1$ is the eigenvector associated with the nonzero eigenvalue. By using (11), $M_\Lambda(t \mid \mathbf{H})$ becomes

$$M_\Lambda(t \mid \mathbf{H}) = \prod_{b=1}^{B} e^{(t+t^2)\frac{1}{N_{0,b}}|w_b|^2 \|\mathbf{s}_b - \hat{\mathbf{s}}_b\|^2}. \tag{13}$$

We then approximate the PEP using the Chernoff bound with $t = -1/2$, which yields

$$f(\mathbf{s}, \hat{\mathbf{s}}) \approx f_{\mathrm{CB}}(\mathbf{s}, \hat{\mathbf{s}}) = \prod_{b=1}^{B} e^{-\gamma_b \frac{\|\mathbf{s}_b - \hat{\mathbf{s}}_b\|^2}{4\sigma_x^2}}, \tag{14}$$

where the effective signal-to-noise ratio (SNR) γ_b is defined as

$$\gamma_b \triangleq \frac{|w_b|^2 \sigma_x^2}{N_{0,b}} \tag{15}$$

and σ_x^2 denotes the variance of $\mathbf{x}$.

B. Illustration of the Convergence with Central Limit Theorem

Since $\mathbf{w}_b$ is a weighted sum of R complex independent random variables, the central limit theorem can be used to prove that both $\mathrm{Re}\{w_{b,r}\}$ and $\mathrm{Im}\{w_{b,r}\}$ converge to Gaussian random variables as $R \to \infty$. The convergence behavior is illustrated in Fig. 2, where the empirical PDFs of $\mathrm{Re}\{w_{b,r}\}$ and $\mathrm{Im}\{w_{b,r}\}$ for $K = 2$ and $\sigma_g^2 = 1$ are depicted, together with the PDF of the Gaussian random variable $\mathcal{N}(0, 1/2)$. We see that for large R, $\mathrm{Re}\{w_{b,r}\}$ and $\mathrm{Im}\{w_{b,r}\}$ approach a Gaussian distribution, illustrating the effect of the central limit theorem.

C. Derivation of the AF

The AF, defined as

$$\mathrm{AF} \triangleq \frac{E[\gamma_b^2] - E[\gamma_b]^2}{E[\gamma_b]^2}, \tag{16}$$

was originally introduced as a measure of the severity of the fading channel. In [14], the AF is generalized to describe the system behavior when signal processing techniques and channel statistics are included, and thus is a convenient and powerful performance criterion. Roughly speaking, the higher the AF, the worse the error rate performance. For example, the AWGN channel, the Rayleigh fading channel, and the K-product Rayleigh fading channel yield $\mathrm{AF} = 0$, $\mathrm{AF} = 1$ and $\mathrm{AF} = 2^K - 1$, respectively [10].

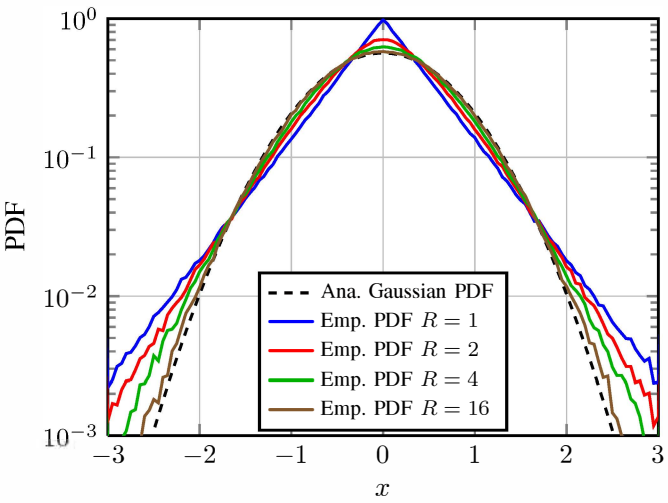

Fig. 2. Empirical PDFs of $\mathrm{Re}\{w_{b,r}\}$ and $\mathrm{Im}\{w_{b,r}\}$ with $K = 2$ and $\sigma_g^2 = 1$, and PDF of a Gaussian random variable $\mathcal{N}(0, 1/2)$.

To compute the AF in our case, we first expand $|w_b|^2$ as

$$|w_b|^2 = \sum_{r=1}^{R} |u_{b,r}|^2 |h_{b,r}|^2 + 2 \sum_{r_1=1}^{R} \sum_{r_2=r_1+1}^{R} |u_{b,r_1}||u_{b,r_2}||h_{b,r_1}||h_{b,r_2}| \cos(\theta_{b,r_1} - \theta_{b,r_2}), \tag{17}$$

where $\theta_{b,r}$ denotes the phase of $h_{b,r}$ and $u_{b,r}$ is the rth entry of $\mathbf{u}_b$. We can compute the first moments of the random variables $|h_{b,r}|$ under the assumption that $|g_{b,r,k}|$ are i.i.d. Rayleigh random variables, whose moments are listed in [14]. We obtain

$$E[|h_{b,r}|] = \prod_{k=1}^{K_r} E[|g_{b,r,k}|] = \left(\frac{\pi \sigma_g^2}{4}\right)^{K_r/2}, \tag{18}$$

$$E\left[|h_{b,r}|^2\right] = \prod_{k=1}^{K_r} E\left[|g_{b,r,k}|^2\right] = \left(\sigma_g^2\right)^{K_r}, \tag{19}$$

$$E\left[|h_{b,r}|^4\right] = \prod_{k=1}^{K_r} E\left[|g_{b,r,k}|^4\right] = 2^{K_r}\left(\sigma_g^2\right)^{2K_r}, \tag{20}$$

Next, consider the random variables $\cos(\theta_{b,r_1} - \theta_{b,r_2})$. Since $\theta_{b,r} = \sum_{k=1}^{K_r} \theta'_{b,r,k}$ with $\theta'_{b,r,k} \sim \mathcal{U}(-\pi, \pi)$ being the phase of $g_{b,r,k}$, where $\mathcal{U}(-\pi, \pi)$ is the uniform distribution with support $[-\pi, \pi]$, then $\cos(\theta_{b,r_1} - \theta_{b,r_2})$ is an arcsine-distributed random variable with support $[-1, +1]$ and first and second moments

$$E[\cos(\theta_{b,r_1} - \theta_{b,r_2})] = 0, \tag{21}$$

$$E\left[\cos^2(\theta_{b,r_1} - \theta_{b,r_2})\right] = \frac{1}{2}. \tag{22}$$

Since $|h_{b,r}|$ and $\theta_{b,r}$ are independent, using (17) we can

compute the mean value of SNR

$$E\left[\gamma_b\right] = \frac{\sigma_x^2}{N_{b,0}} E\left[|w_b|^2\right] \overset{(a)}{=} \frac{\sigma_x^2}{N_{b,0}} \sum_{r=1}^{R} |u_{b,r}|^2 \left(\sigma_g^2\right)^{K_r}, \quad (23)$$

where (a) follows from (18), (19), and (21). To calculate $E\left[\gamma_b^2\right]$, $|w_b|^4$ is first expanded as

$$|w_b|^4 = \left(\sum_{r=1}^{R} |u_{b,r}|^2 |h_{b,r}|^2\right)^2 + 2\left(\sum_{r=1}^{R} |u_{b,r}|^2 |h_{b,r}|^2\right) \times \left(2\sum_{r_1=1}^{R}\sum_{r_2=r_1+1}^{R} |u_{b,r_1}||u_{b,r_2}||h_{b,r_1}||h_{b,r_2}| \cos\left(\theta_{b,r_1} - \theta_{b,r_2}\right)\right) + \left(2\sum_{r_1=1}^{R}\sum_{r_2=r_1+1}^{R} |u_{b,r_1}||u_{b,r_2}||h_{b,r_1}||h_{b,r_2}| \cos\left(\theta_{b,r_1} - \theta_{b,r_2}\right)\right)^2. \quad (24)$$

Then, we have

$$E\left[\gamma_b^2\right] \overset{(a)}{=} \left(\frac{\sigma_x^2}{N_{b,0}}\right)^2 \left(E_{\mathbf{h}_b}\left[\left(\sum_{r=1}^{R} |u_r|^2 |h_{b,r}|^2\right)^2\right] + E_{\mathbf{h}_b}\left[2\sum_{r_1=1}^{R}\sum_{r_2=r_1+1}^{R} |u_{r_1}|^2 |u_{r_2}|^2 |h_{b,r_1}|^2 |h_{b,r_2}|^2\right]\right) \overset{(b)}{=} \left(\frac{\sigma_x^2}{N_{b,0}}\right)^2 \left(\sum_{r=1}^{R} |u_{b,r}|^4 2^{K_r} \left(\sigma_g^2\right)^{2K_r} + 4\sum_{r_1=1}^{R}\sum_{r_2=r_1+1}^{R} |u_{b,r_1}|^2 |u_{b,r_2}|^2 \left(\sigma_g^2\right)^{K_{r_1}+K_{r_2}}\right), \quad (25)$$

where (a) follows from (21) and (22), and (b) from (19) and (20).

To shed light on the influence of K and R on the AF, we make the assumption that the variance of the link gain is normalized, i.e., $\sigma_g^2 = 1$. Thus, (23) and (25) can be simplified to

$$E\left[\gamma_b\right] = \frac{\sigma_x^2}{N_{b,0}},$$
$$E\left[\gamma_b^2\right] \overset{(a)}{=} \left(\frac{\sigma_x^2}{N_{b,0}}\right)^2 \left(2 + \sum_{r=1}^{R} |u_{b,r}|^4 (2^{K_r} - 2)\right), \quad (26)$$

where (a) follows from

$$1 = \left(\sum_{r=1}^{R} |u_{b,r}|^2\right)^2 = \sum_{r=1}^{R} |u_{b,r}|^4 + 2\sum_{r_1=1}^{R}\sum_{r_2=r_1+1}^{R} |u_{b,r_1}|^2 |u_{b,r_2}|^2. \quad (27)$$

The AF takes the form

$$\mathrm{AF} = 1 + \sum_{r=1}^{R} |u_{b,r}|^4 (2^{K_r} - 2) \quad (28)$$

and is upper bounded by

$$\mathrm{AF} \leq 2^{\max_{r=1,\ldots,R}\{K_r\}} - 1. \quad (29)$$

In the special of all relay paths having the same number of links, we may drop the subscript r of K_r, which yields the lower bound

$$\mathrm{AF} \geq 1 + \frac{2^K - 2}{R} \quad (30)$$

as a consequence of the Cauchy-Schwarz inequality

$$R\sum_{r=1}^{R} |u_{b,r}|^4 \geq \left(\sum_{r=1}^{R} |u_{b,r}|^2\right)^2 = 1. \quad (31)$$

Note that in (30) equality holds when $u_{b,r} = R^{-1/2}$ for $r = 1, \ldots, R$.

Since the AF of the K-product Rayleigh fading is enhanced by the PTC and lower bounded by the AF of Rayleigh fading when $R \to \infty$, by using the PDF of Rayleigh fading and the PDF of cascaded fading, expressed by the Meijer G-function [15], [16]

$$p_{|h|}(x) = G_{0,K}^{K,0}\left[x^2 \middle| \begin{matrix} - & - \\ 1/2 & \ldots \quad 1/2 \end{matrix}\right], \quad (32)$$

the PEP approximation $f_{\mathrm{CB}}(\mathbf{s}, \hat{\mathbf{s}})$ in (14) is bounded by

$$\prod_{b=1}^{B}\left(1 + \frac{\|\mathbf{s}_b - \hat{\mathbf{s}}_b\|^2}{4\sigma_x^2}\gamma_b\right)^{-1} \leq f_{\mathrm{CB}}(\mathbf{s}, \hat{\mathbf{s}}) \leq \prod_{b=1}^{B} G_{K,1}^{1,K}\left[\frac{\|\mathbf{s}_b - \hat{\mathbf{s}}_b\|^2}{4\sigma_x^2}\gamma_b \middle| \begin{matrix} 0 & \ldots & 0 \\ & 0 & \end{matrix}\right]. \quad (33)$$

The last term in (33) expresses the performance in terms of coding and diversity gains when the channel statistics are those of a K-product Rayleigh fading. Since path–time codes reshape the channel statistics, the resulting PEP is better, as it approaches the PEP Chernoff bound corresponding to a Rayleigh fading channel when $R \to \infty$.

IV. Simulation Results

In this section, the performance of the end-to-end PTC transmission is evaluated by computer simulation, done to validate our analysis.

Fig. 3 plots the AF with DFT-based PTC [7] with unity code rate. Here, we only consider the error event whose Hamming distance between $\mathbf{x}$ and $\hat{\mathbf{x}}$ is one. In this case, $u_{b,r} = R^{-1/2}$, and the lower bound in (30) holds with equality. We can see that, for small K, the AF quickly drops to unity, which is the AF value of Rayleigh fading channels. However, for $K = 6$, the AF decreases slowly, since this value is exponentially proportional to K and linearly inversely proportional to R as shown in (30).

The bit error rates (BERs) of end-to-end PTC transmission for $R = 2$ and $R = 4$ are illustrated in Fig. 4(a) and Fig. 4(b). For $R = 4$, the performance loss caused by cascading fading channels decreases. For example, the BER gaps between the system with Rayleigh fading ($K = 1$) and cascaded fading ($K = 6$) are 22 dB and 10 dB for the case with $R = 2$ and $R = 4$, respectively.

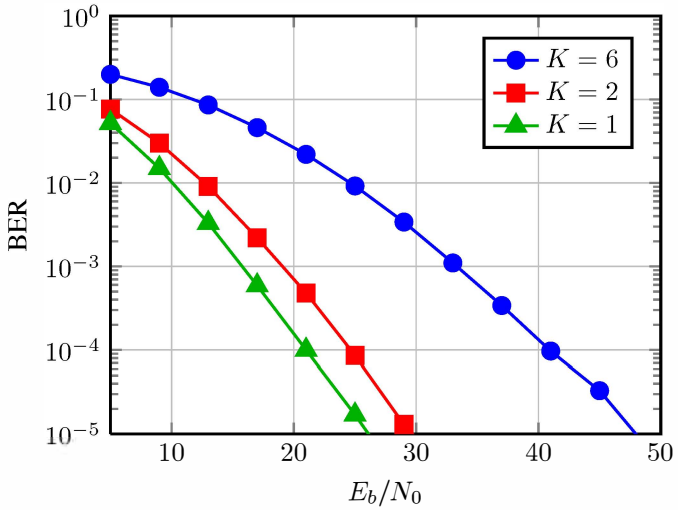

(a) $R = 2$

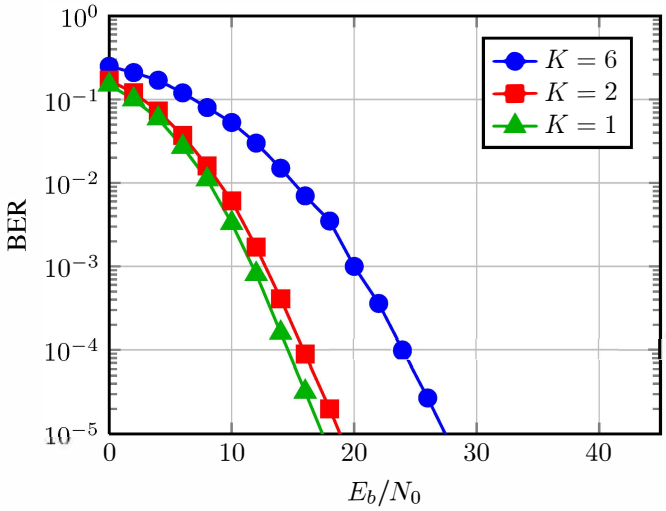

(b) $R = 4$

Fig. 4. BER comparisons of the end-to-end PTC transmission with various number of links K and relay paths R; QPSK modulation is adopted.

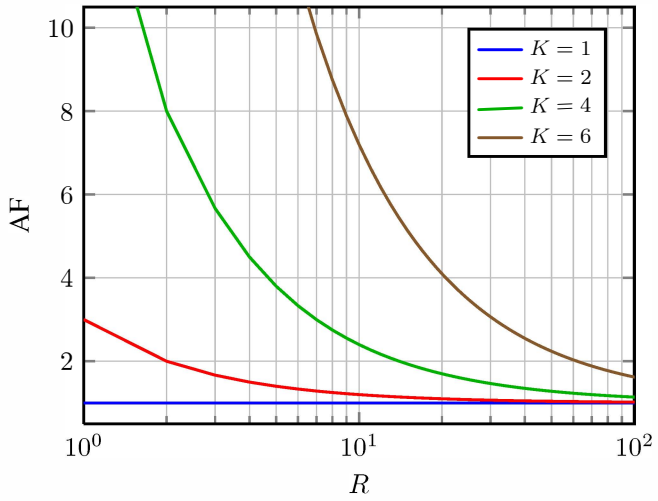

Fig. 3. AF of the end-to-end PTC transmission with various number of links K and relay paths R.

V. Conclusion

In this paper, we have shown that in addition to the diversity and coding gains achieved by space–time codes, path–time codes can reshape the channel statistics of end-to-end PTC transmission from cascaded-Rayleigh fading to Rayleigh fading. This effect was numerically verified and analytically studied through the calculation of the AF. The closed-form expression of the AF we have obtained indicates the influence on performance of the number of relay paths and the number of links, and consequently can be used as a design tool. It should be emphasized that this result is also applicable to more general distributed STC-based transmissions [1]–[4] in relay networks.

Acknowledgement

E. B.'s work was supported by Project TEC2012-34642 and by the Distinguished Scientist Fellowship Program at King Saud University. K.-C. Chen was supported by the National Science Council under the contract NSC102-2221-E-002-016-MY2. C.-H. Lee was supported by the National Science Council under the contract NSC102-2219-E-001-001.

References

[1] J. N. Laneman and G. W. Wornell, "Distributed space–time-coded protocols for exploiting cooperative diversity in wireless networks," *IEEE Trans. Inf. Theory*, vol. 49, no. 10, pp. 2415–2425, Oct. 2003.

[2] R. U. Nabar, H. Bölcskei, and F. W. Kneubühler, "Fading relay channels: Performance limits and space–time signal design," *IEEE J. Sel. Areas Commun.*, vol. 22, no. 6, pp. 1099–1109, Aug. 2004.

[3] Y. Jing and B. Hassibi, "Distributed space–time coding in wireless relay networks," *IEEE Trans. Wireless Commun.*, vol. 5, no. 12, pp. 3524–3536, Dec. 2006.

[4] F. Oggier and B. Hassibi, "An algebraic coding scheme for wireless relay networks with multiple antenna nodes," *IEEE Trans. Signal Process.*, vol. 56, no. 7, pp. 2957–2966, Jul. 2008.

[5] B. Rankov and A. Wittneben, "Distributed spatial multiplexing in wireless networks," in *Proc. Asilomar Conf. on Signals, Systems, and Computers*, Jun. 2004.

[6] I.-W. Lai, C.-H. Lee, and K.-C. Chen, "A virtual MIMO path-time code for cognitive ad hoc networks," *IEEE Commun. Lett.*, vol. 17, no. 1, pp. 4–7, Jan. 2013.

[7] I.-W. Lai, C.-L. Chen, C.-H. Lee, K.-C. Chen, and E. Biglieri, "End-to-end virtual MIMO Transmission in ad hoc cognitive radio networks," *IEEE Trans. Wireless Commun.*, 2014, to be published.

[8] M. K. Marina and S. R. Das, "On-demand multipath distance vector routing in ad hoc networks," in *Proc. 2001 IEEE Int. Conf. on Network Protocol (ICNP)*, Nov. 2001.

[9] P. Djukic and S. Valaee, "Reliable packet transmissions in multipath routed wireless networks," *IEEE Trans. Mobile Comput.*, vol. 5, no. 5, pp. 548–559, May 2006.

[10] G. K. Karagiannidis, N. C. Sagias, and P. T. Mathiopoulos, "N*Nakagami: A novel stochastic model for cascaded fading channels," *IEEE Trans. Commun.*, vol. 55, no. 8, pp. 1453–1458, Aug. 2007.

[11] W.-C. Ao and K.-C. Chen, "End-to-end HARQ in cognitive radio network," in *Proc. IEEE Wireless Commun. and Networking Conf. (WCNC)*, Jul. 2010, pp. 1–6.

[12] P.-Y. Chen, W.-C. Ao, and K.-C. Chen, "Rate-delay enhanced multipath transmission scheme via network coding in multihop networks," *IEEE Commun. Lett.*, vol. 16, no. 3, pp. 281–283, Mar. 2012.

[13] V. Tarokh, N. Seshadri, and A. R. Calderbank, "Space–time codes for high data rate wireless communication: Performance criterion and code construction," *IEEE Trans. Inf. Theory*, vol. 44, no. 2, pp. 744–765, Mar. 1998.

[14] M. Simon and M. S. Alouini, *Digital Communications over Fading Channels*. John Wiley & Sons, 2005.

[15] J. Salo, H. M. El-Sallabi, and P. Vainkainen, "The distribution of the product of independent Rayleigh random variables," *IEEE Trans. Antennas Propag.*, vol. 54, no. 2, pp. 639–643, Feb. 2006.

[16] I. S. Gradshteyn and I. M. Ryzhik, *Table of Integrals, Series and Products*, 7th ed. New York: Academic, 2007.